Journal of Magnetism and Magnetic Materials 374 (2015) 148–152

Contents lists available at ScienceDirect

Journal of Magnetism and Magnetic Materials

journal homepage: www.elsevier.com/locate/jmmm

First principles calculation of magnetic order in a low-temperature phase of the iron ludwigite

M. Matos [a,*], J. Terra [b], D.E. Ellis [b,c], A.S. Pimentel [d]

[a] Departamento de Física, PUC-Rio, Rua Marques de São Vicente, 225, Gávea, Rio de Janeiro, RJ 22453-970, Brazil
[b] Centro Brasileiro de Pesquisas Físicas, Rio de Janeiro, RJ, Brazil
[c] Northwestern University, Evanston, IL, USA
[d] Departamento de Química, PUC-Rio, Rua Marques de São Vicente, 225, Gávea, Rio de Janeiro, RJ 22453-970, Brazil

ARTICLE INFO

Article history:
Received 8 October 2013
Received in revised form
25 February 2014
Available online 13 August 2014

Keywords:
Fe ludwigite
Theory
DFT
Non-collinear spin
Magnetic order

ABSTRACT

The magnetic order of a low-temperature dimerized phase of $Fe_3O_2BO_3$ is investigated through a density functional approach which considers full non-collinear spin–spin interactions, focusing on the 15 K crystalline structure. It is found that Fe spins in the $(Fe–Fe)^{5+}$ dimer, formed during the room temperature structural change of $Fe_3O_2BO_3$, are parallel and have little freedom to rotate under interaction with neighbor Fe atoms. While the Fe dimer behaves as a heavy single magnetic unit the spin magnetic moment of the third Fe^{3+} atom of the Fe *triad* has, on the contrary, much more freedom to rotate. This is responsible for a canted spin ordering, revealed by a rotation of $\sim 80^\circ$ of the trivalent Fe spin relative to the spin orientation of the dimer, due to spin–spin interaction with divalent Fe atoms outside the *triad*. Canting is thus seen to be responsible for the very low net magnetization, experimentally observed in this compound ($T < 40$ K).

1. Introduction

The renewed interest in the study of ludwigite compounds observed in the last decades was initially motivated by the low dimensionality of their crystal structure and its similarity with spinels [1–3]. After the discovery of a structural change in the Fe ludwigite [4,5], research has been mainly focused on understanding the mechanisms that cause the atomic instabilities. The structural change occurs at temperature $T_S = 283$ K and consists of an orthorhombic–orthorhombic transition that affects essentially a group of three Fe atoms. This iron *triad* stacks in one crystalline direction, forming a quasi-one-dimensional substructure that is responsible for the most interesting physical properties of this material [6–11].

Ludwigite is a metal oxo-borate of formula unit $M'_2MO_2BO_3$, where M′ and M are di- and trivalent metals. The crystalline structure consists of corrugated planes of oxygen octahedra filled with metals occupying 4 distinct crystal sites [6,12]. Trigonal BO_3 groups hold the planes together. Fig. 1 shows a polyhedral view of the $a \times b$ face of ludwigite, which has a flat orthorhombic unit cell ($a \sim 9$ Å, $b \sim 12$ Å and $c \sim 3$ Å), with 4 formula units. Considering the 4 different positions occupied by iron and 5 positions of oxygen atoms, the formula per unit cell of the mixed valence Fe ludwigite can be written as $(Fe4Fe2Fe4)_2(Fe3\ Fe1Fe3)_2(O2O4)_4(BO1O3O5)_4$. There are two Fe *triads*, 424 and 313, the former being associated with the complex behavior of this ludwigite, including the structural transition. In the high temperature phase the Fe2–Fe4 distance is 2.78 Å, the shortest observed in the Fe system of $Fe_3O_2BO_3$. Due to the structural transition, site 4 splits into 4a and 4b and inter-atomic distances change to 2.94 Å (Fe4b–Fe2) and 2.60 Å (Fe4a–Fe2). The transition could therefore be seen as a dimerization in the *triad*, with Fe4a-Fe2 forming the Fe dimer. Rietveld refinements show a doubling of the *c*-axis in the low temperature dimerized phase with alternation of the Fe2-Fe4a dimer along the *c*-axis [5]. Besides Fe ludwigite, $Co_3O_2BO_3$ is the only other homo-metallic ludwigite synthesized so far [13]. However, despite the strong similarity between the two mixed valence compounds, no structural transition was observed in the cobalt ludwigite [14,15].

Atomic instabilities were observed in other 2–3 mixed valence Fe oxides such as the spinel magnetite and the homo-metallic warwickite, Fe_2OBO_3, a different type of oxo-borate [1,16,18]. Both compounds undergo an orthorhombic–monoclinic transition driven by charge localization which forms a Wigner crystal phase [16–20]. Each of these materials exhibits one magnetic transition; Fe_3O_4 is ferromagnetic below $T_F = 858$ K and the warwickite becomes anti-ferromagnetic at $T_{AF} = 155$ K. No clear indication was found of interplay between charge localization and magnetism in these materials. Charge localization in magnetite occurs at 120 K (well below the magnetic transition) and in warwickite at

* Corresponding author. Tel.: +55 21 3527 1263.
E-mail address: maria.matos@fis.puc-rio.br (M. Matos).

http://dx.doi.org/10.1016/j.jmmm.2014.08.025
0304-8853/

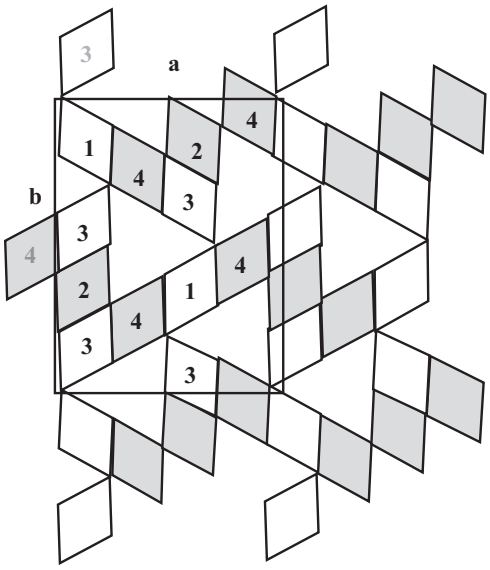

Fig. 1. Octahedral representation of $Fe_3O_2BO_3$, projected in the $a \times b$ plane, with unit cell indicated. Fe sites of the *triads* 424 and 313 are shown.

317 K (well above the magnetic transition) [16]. In $Fe_3O_2BO_3$, however, magnetism and charge ordering present more subtle behaviors that seem to be related, even though structural and magnetic transition temperatures differ. The first magnetic transition that occurs at 112 K, for instance, consists of an AF magnetic ordering which takes place mainly in the 424 *triad*, although Fe3 also begins to order magnetically in this temperature [3,8,9]. In the range 70–40 K, weak ferromagnetism was suggested with the inclusion of Fe1 in the magnetic order. Below 40 K the whole Fe spin system is ordered in a so-called 3D AF phase [3,9]. Thus, differently from magnetite and warwickite, in ludwigite there are three distinct magnetic phases, instead of one, all below the structural transition.

Formally, valences in the 424 group are (3+)(2+)(3+). However, like magnetism in the ludwigite, charge distribution presents different regimes, as seen from Mössbauer data obtained independently by Douvalis et al. [8] and Larrea et al. [9]. Results of both studies confirm the presence of divalent atoms attributed to Fe1 and Fe3 over a large temperature range (from 4 K to above 450 K). In the 424 group, good agreement is obtained within both studies for $T > 40$ K. Above 283 K there are two intermediate valences in the 424 *triad*, one close to 3^+ and the other close to 2+ associated to Fe4 and Fe2, respectively; at the structural transition (283 K) Fe4a reaches a valence close to that of Fe2 ($\sim +2.5$) while the charge of Fe4b approaches 3+, consistent with the dimerized structure. When magnetism sets in (112 K), the charge distribution continues to change although more smoothly. Between 112 K and 40 K there is an increasing tendency of uniformization of valences in the dimer, and that of Fe4b progressively approaching 3+.

Below 40 K results obtained by Douvalis et al. [8] and Larrea et al. [9] differ, both data confirming a tendency of the valences of the 424 *triad* to collapse into only two, pointing however to two possible arrangements $(Fe4b^{3+})(Fe2–Fe4a)^{5+}$ [8] and [9] $(Fe4b)^{2.5+}(Fe2)^{2+}(Fe4a)^{2.5+}$. More recently [11], from neutron diffraction data at 10 K, it was suggested that magnetic moments in the 424 *triad* are aligned ferromagnetically (F). AF alignment along *c* was assumed to satisfy the observed low magnetization of the sample. Earlier it had been suggested that, at very low temperatures, magnetic moments in the *triad* aligned antiferromagnetically [1,18]. Both studies find that magnetic moments in the group of Fe1 are opposite to those of Fe3, both perpendicular to the moments in the 424 *triad*. These results could be related to the interplay between magnetism and charge ordering in the 424 group since ferromagnetic alignment in a pair of Fe atoms favors electron hopping, leading to intermediate valence.

Theoretical research on $Fe_3O_2BO_3$ has been mainly based on one electron tight binding-based methodology. Realistic geometry-dependent electron–lattice interactions were studied by using the extended Hückel methodology with high spin band electronic configuration; local geometrical distortions of the oxygen octahedra were found to be related to the opening of a gap at the Fermi level of the minority spin band of the 424 *triad* [21]. The same methodology was used in an extensive study of spin exchange in both crystalline structures of $Fe_3O_2BO_3$ [22]. It was suggested that neighbor Fe spins are probably anti-parallel, independent of the pair. Tight binding models with infinite-U electron–electron repulsion on a three-leg ladder (3LL) system of Fe atoms have considered the possibility of Peierls instabilities being manifested in the structural transition [23]. More recently, Vallejo and Avignon [24]and Vallejo [25] included double and super-exchange terms in a tight binding hamiltonian to investigate the behavior of an itinerant electron in a trivalent, high-spin Fe triple describing the Fe4–Fe2–Fe4 rung. Phase diagrams relating spin exchange J and hopping parameters t provided general predictions of possible spin arrangements. They found that for reasonable parameters there is a tendency of ferromagnetic alignment in each rung, according to experimental predictions of Bordet and Suard [11]. These authors also suggest the presence of spin canting in the 424 *triad*.

In spite of considerable effort toward the understanding of the electronic and magnetic structure in the homo-metallic Fe ludwigite, a clear picture of the complex behavior of this material has not yet been given. A more detailed theoretical description of the system's magnetism could provide new insight into the behavior of this complex material. Thus we decided to do a first principles theoretical study of this compound by choosing the low-temperature dimerized phase of $Fe_3O_2BO_3$ for the following reasons: (i) neutron diffraction data and refined crystalline structure are available at $T = 10$ K and 15 K, respectively, (ii) in the range $\sim 5 – \sim 40$ K, the magnetic arrangement and charge distribution are not expected to change considerably and (iii) it is a starting point to understand the more complex behavior around the structural transition. We use a first principles density functional theory taking into account, self-consistently, non-collinear spin–spin interactions. This is done by including in the exchange correlation functional the magnetization density, according to the methodology proposed by Hobbs et al. [26], available in the VASP computational code [27].

2. Computational details

The non-collinear spin-polarized electronic structure of Fe-ludwigite at 15 K has been obtained with periodic band-structure calculations using the first principles quantum-mechanical electronic structure density functional theory (DFT) program VASP [27]. The projector augmented wave potential and a plane wave basis set were employed using the Perdew–Burke–Emzerhof generalized gradient approximation (PAW-PBE) to describe the exchange and correlation. The Brillouin zone integration was performed using K-points grids of $2 \times 2 \times 3$ up to $4 \times 4 \times 5$ mesh within the Monkhorst–Pack scheme for electronic optimization and total energy calculations. Convergence is considered to be achieved when the total energy between two iterations is smaller than 1 meV. The electrons described as core in the PAW potentials are those composed of $[Ne]3s^2$ for Fe, leaving $3p^6 3d^7 4s^1$ valence electrons and [He] for both B and O leaving $2s^2 2p^1$ and $2s^2 2p^4$ valence electrons for B and O, respectively. Lattice parameters and

atomic positions were kept fixed with values given in Tables 1 and 2 of Ref. [5] for Fe-ludwigite at 15 K. Since the *c*-axis is doubled at the structural transition, we use the notation $1 \times 1 \times 2$ to represent the unit cell at 15 K.

3. Results

In this section, results obtained from calculations on the dimerized phase of $Fe_3O_2BO_3$ are discussed. Full non-collinear spin–spin interactions are allowed between all the atoms of the system. Initial atomic magnetic moments must be given as input to VASP for the definition of spin interaction terms of the density functional. Special consideration is given to this spin part of the input, since a clear criterion has not yet been established for the ludwigites to insure reliability of the calculated ground state. In general we have adopted, as input, a configuration based on magnetic moments for Fe, with oxygen and boron assumed to have zero initial magnetization. The equilibrium values are then determined as a result of the self-consistent optimization process, giving the final spin configuration of the system. In order to validate the conclusions, several calculations were performed by using different Fe spin arrangements as input (input models).

The first input model considered, IM1, was taken from the Fe spin configuration (orientation and absolute values of $\boldsymbol{\mu}$(Fe)) experimentally determined for $Fe_3O_2BO_3$ at 10 K [11], according to which Fe4a, Fe2 and Fe4b magnetic moments are arranged ferromagnetically, whereas between neighboring rungs along *c* the alignment is AF. In this arrangement, the 313 *triad* has spins anti-parallel inside the rungs but the order along *c* is ferromagnetic. This configuration is schematically indicated by arrows in Table 1. In units of the Bohr magneton, μ_B, the actual values are $\boldsymbol{\mu}$(Fe2)=$\boldsymbol{\mu}$(Fe4a)=$\boldsymbol{\mu}$(Fe4b)=(0.0,3.3,0.0), $\boldsymbol{\mu}$(Fe1)=(3.3,0.0,0.0), and $\boldsymbol{\mu}$(Fe3)=(−4.0,0.0,0.0). This initial arrangement leads to a total input magnetization per unit cell $\mathbf{M}=(-18.8,0.0,0.0)$. The net M_x -component is due to the presence of twice as many Fe3 atoms as that of Fe1 per unit cell. Results obtained with IM1 show significant canting of spin in the 424 *triad*, characterized by the rotation of $\boldsymbol{\mu}$(Fe4b) toward the direction of magnetic moments of the 313 *triad*. As a consequence of canting the magnetization drops to $\mathbf{M}=$(3.82,0.01,0.04), which is closer to the experimental observation of very low magnetization below ∼40 K [3,8]. Table 2 shows a simplified picture of the final equilibrium orientations and magnitudes of $\boldsymbol{\mu}$(Fe) in both *triads*. The obtained magnitudes μ vary between 3.3 and 3.4 and show no significant differences between sites. It is clear that spin canting is significant in Fe4b, whose magnetic moment $\boldsymbol{\mu}$(Fe4b) rotates toward the *x* axis by $\theta_{4b}=80^\circ$, while $\boldsymbol{\mu}$(Fe4a) ($\theta_{4a}=15$–17°) and $\boldsymbol{\mu}$(Fe2) ($\theta_2=5^\circ$) show much smaller deviations from *y*. Slight deviations from *x* are observed in Fe3, with $\alpha_3=15^\circ$. Since the bond length of the pair Fe4b–Fe2 is larger than that of Fe2–Fe4a, Fe4b could be expected to change orientation more freely upon interaction with Fe1 and Fe3 and this is confirmed by the spin canting in Fe4b. Contrarily spins of Fe2 and Fe4a keep their orientation nearly unchanged, showing that this pair behaves as a single, stiff unit. This result provides confirmation of Fe2–Fe4a dimerization in this temperature range.

Other input models shown in Table 1 make changes in the spin orientations of the 424 *triad*. To compensate non-vanishing M_x of IM1, IM2 was considered; it differs from IM1 merely with respect to the spin orientation of Fe4b, assumed to lie on the *x*-axis, being thus aligned with Fe1. By appropriately defining $\boldsymbol{\mu}$(Fe4b) the input magnetization was made to vanish, to approach the low experimental values. As noted in Table 2, results obtained with IM2 reproduce the ground state configuration of IM1 with $\theta_{4b}=78^\circ$. Other atomic magnetic moments and $\mathbf{M}=$(2.76,0.01,0.03) were also found to be very close to the former calculated values. The IM2 ground state energy is 2.07 meV above IM1, which is on the order of thermal energy at 15 K, kT=1.3 meV.

We have also considered the case IM3 in which $\boldsymbol{\mu}$(Fe4b) is anti-parallel to the magnetic moments of the dimer pair Fe4a–Fe2. As seen in Tables 1 and 2, the final magnetization and spin configuration closely reproduce the results found with IM1. Spin canting in site 4b ($\theta_{4b}=83$–88°) is only slightly larger probably due to the initial orientation of $\boldsymbol{\mu}$(Fe4b), anti-parallel to the dimer. In the self-consistent iteration the rotation $\boldsymbol{\mu}$(Fe4b) was effectively larger, 112°, to achieve the equilibrium value. $\Delta E=E$(IM3)–E(IM1) was found to be 6.1 meV for this model, in the range of kT∼1.3 meV. Results found with the input models IM1–IM3 just lead to ground state energies thermally comparable and nearly equal equilibrium spin configurations.

In order to check further the stability of the former results, other models for input spin configuration were considered by redefining spin orientations and magnitudes in both 424 and 313 *triads*. Three general criteria were adopted, giving rise to four groups of IM. In the first group, the initial magnitudes of some or all $\boldsymbol{\mu}$(Fe) are defined as half of those considered in IM1. In this group one obtains ΔE varying between ∼30 meV and ∼70 meV, one order of magnitude larger than kT. The second group investigated the possibility that all spins point along the same direction, namely *x* or *y*, while keeping the relative ferromagnetic or anti-ferromagnetic alignment as that of

Table 1
Description of input models for non-collinear spin calculations and results obtained for $\Delta=E-E(\mathbf{1})$ and magnetization. *E* is the calculated energy per unit cell. Spin axis *x*, *y*, *z* are assumed to be parallel to lattice directions *a*, *b*, *c*, respectively. Magnetic moments in units of μ_B.

Input model	**(4b 2 4a) (4a 2 4b)**	**(3 1 3)**	spinaxis	ΔE (meV)	Magnetization (initial) (converged)
IM1	(↑ ↑ ↑) (↓ ↓ ↓)	(← → ←) (← → ←)	y, x	0.0	(-18.8, 0.0, 0.0) (3.82,0.01,0.04)
IM2	(→ ↑ ↑) (↓ ↓ →)	"	"	2.065	(0.0, 0.0, 0.0) (2.76,0.01,0.03)
IM3	(↑ ↓ ↓) (↑ ↑ ↓)	"	y, x	6.075	(-13.2, 0.0, 0.0) (4.52,0.24,-0.04)
IM4	(↓ ↑ ↓) (↑ ↓ ↑)	"	y, x	2950	(-18,8 0.0, 0.0) (-21.60,-0.23,-0.05)

Table 2
Orientation and magnitude μ of Fe magnetic moments calculated from input models described in Table 1. Magnetic moments in units of μ_B. Angles θ and α: see definition in Fig. 2.

input –model	(4b 2 4a) (4a 2 4b)	(31 3)	spinaxis	α --- θ
IM1	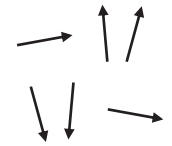	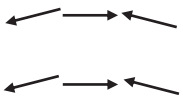		Fe1: 0° Fe3: 15° --- Fe2: 5° Fe4a: 15° – 17° Fe4b: 80°
IM2	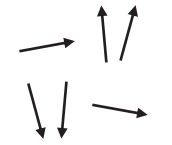	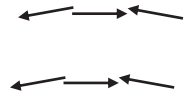		Fe1: 0° Fe3: 10° --- Fe2: 7° Fe4a: 16° Fe4b: 78°
IM3	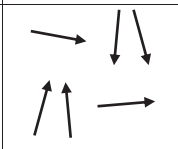	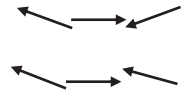		Fe1: 0° Fe3: 21° – 25° --- Fe2: 7° Fe4a: 14° – 16° Fe4b: 83° – 88°
IM4	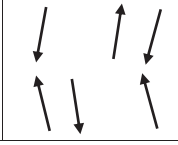	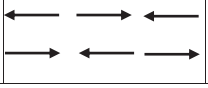		Fe1: 0° Fe3: 0° --- Fe2: 7° – 13° Fe4a: 9° – 20° Fe4b: 15° – 19°

IM1. The converged energy per unit cell was found to be ~400 meV larger than E(IM1), thus two orders of magnitude larger than kT. In the third group we examined the consequences of starting the iteration process with a spin configuration where one Fe3 per unit cell is rotated 180° pointing toward $+x$, thus giving zero initial magnetization for the system. After convergence one gets $\Delta E \sim 790$–840 meV, twice as high as in the second group. Particularly, this result strongly supports the AF 313 rung alignment. The fourth group repeats the criteria used in each of the three former groups, except that spins in the Fe2–Fe4a dimer are assumed to be anti-parallel. The converged energies were found to be much higher than E(IM1), giving $\Delta E = 2$–3 eV, three orders of magnitude above kT. This analysis gives a further support for the results described in the earlier paragraph.

Let us compare IM3, belonging to the optimal group, with IM4, this one taken from the fourth group discussed in the former paragraph. The initial and final spin configurations of IM4 can be found in Tables 1 and 2. It should be noted that the only difference between these two input models (IM3 and IM4) comes from the spin alignment in the Fe2–Fe4a dimer. In IM3, Fe2 and Fe4a have parallel spins while in IM4 they have anti-parallel spins. Non-dimerized Fe4b has its spin anti-parallel to that of Fe2 in both cases. Taking into account that $\Delta E_{\text{parallel}} = 6$ meV (IM3) and $\Delta E_{\text{anti-parallel}} \sim 3$ eV (IM4) with all other spin arrangements equivalent, it could be said that spin flip inside the dimer requires a lot more energy than other changes in spin orientations. Given that there are 4 dimers per unit cell we have an amount of about 800 meV per Fe2–Fe4a dimer, each individual spin flip energy being thus well above kT, at 15 K.

We have examined the effect of reversing the direction of the magnetic moment of one specific Fe3 on the magnetic moments of Fe4b. Changes were significant: instead of the former rotation of ~80° $\boldsymbol{\mu}$(Fe4b) showed smaller rotational angles, varying from 51° to 10°, indicating the loss of local canting in some 4b sites. Other Fe atoms exhibited negligible changes in the rotational behavior.

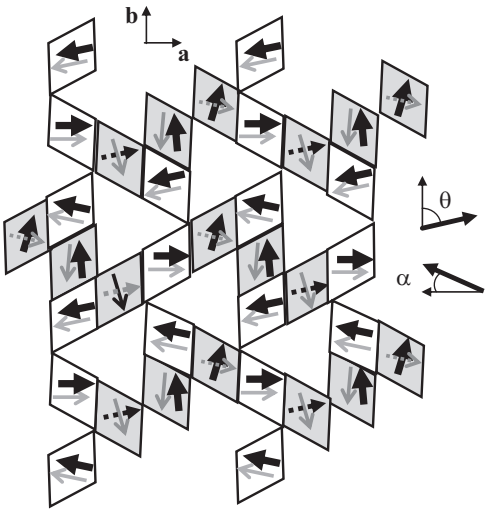

Fig. 2. The distribution of magnetic moments in the polyhedral representation of $Fe_3O_2BO_3$, projected in the $a \times b$ plane. Broken arrows: site 4b; black (gray) arrows: upper(lower) parts of the $1 \times 1 \times 2$ unit cell; θ and α: rotation angles of Fe spins in the 424 and 313 *triads* respectively, with respect to the initial guess of IM2 spin configuration. θ_{4b} determines the amount of spin canting. Gray octahedra indicate the 424 *triads*.

These results clearly indicate that the interaction between Fe3 and Fe4b plays a fundamental role in the magnetic interaction between 424 and 313 *triads*.

By examining the convergence of results with the K points mesh it was found that IM2 turns out to be the best starting point, with the converged system's energy 12.4 meV below IM1. The IM2 converged solution is therefore taken as the best approximation for the ground state of the 15 K structure of $Fe_3O_2BO_3$. With IM3, the only other case worth considering, the system's energy increases with the number of K points. Fig. 2 shows the Fe spin

distribution obtained with the optimal solution. Rotation angles showed negligible differences from the IM2 values of Table 2.

The present study on non-collinear spin–spin interactions in the Fe ludwigite provides a quantitative support for the spin arrangement at 15 K, which comes out to be very similar to that proposed by Vallejo and Avignon [24] by using tight-binding-based methods. Particularly, one obtains a clear description of the (main) 424 *triad* as consisting of two elements: (i) a Fe–Fe dimer which behaves as a single stiff magnetic unit $\boldsymbol{\mu}_{Fe2-Fe4a}$, of magnitude $\sim 6\,\mu_B$ and (ii) an atomic magnetic moment $\boldsymbol{\mu}_{Fe4b}(\sim 3\,\mu_B)$ weakly bound to the dimer and with considerable freedom to rotate.

Taking into consideration that the energy of formation of the ferromagnetic Fe2–Fe4a pair at 15 K is $\sim$30 times the room temperature thermal energy, strongly coupled ferromagnetic Fe2–Fe4a pairs are expected to be formed at higher temperatures as well and influence the magnetic order. However, the mechanisms through which these pairs affect the system´s magnetism above 40 K still remain to be understood.

4. Conclusion

First principles calculations have been performed in the 15 K structural phase of $Fe_3O_2BO_3$ using the density functional methodology with non-collinear spin–spin interactions. By comparing several different initial magnetic configurations for the iteration process of the self-consistent solution a state was found whose total energy is $\sim 10kT$ below those of all other states analyzed, being thus considered as a good approximation for the ground state. The obtained magnetic order is in accordance with the experimental diffraction data of Bordet and Suard [11] with additional spin canting suggested by Vallejo and Anignon. [24]. The present calculations provide quantitative evidence for the magnetic order of the Fe-ludwigite at 15 K, which could be described as follows: (1) there is ferromagnetic order in the Fe_2–Fe4a dimer associated with spin–spin interaction well above kT; (2) Fe4b spin canting was obtained, with a rotation of 78° relative to the magnetic moments of the Fe_2–Fe4a dimer; (3) all spins in the 424 *triad* order anti-ferromagnetically along *c*; and (4) spins of the 313 *triad* are anti-parallel in the $a \times b$ plane rungs and order ferromagnetically along *c*.

It is found that an energy of 800 meV is necessary for the Fe4a–Fe_2 dimer to perform a spin flip from parallel to anti-parallel alignment, showing the pair to behave as a single stable magnetic unit. The 424 *triad* is therefore described as consisting of two almost independent elements. a robust magnetic unit $\boldsymbol{\mu}_{Fe4a-Fe2}$, with little freedom to rotate, plus a more weakly bound atomic magnetic moment $\boldsymbol{\mu}_{Fe4b}$. As a consequence spin canting occurs due to spin–spin interactions in Fe_4b–Fe_3 pairs, which in turn is responsible for lowering the sample magnetization. The magnetic structure of the 424 *triad* is consistent with electron hopping in the dimer pair.

It is expected that strongly coupled ferromagnetic Fe_2–Fe_4a pairs are formed at higher temperatures, thus influencing the magnetic order. More first principles studies must nevertheless be done to understand the details of magnetic interactions in magnetic phases of $Fe_3O_2BO_3$ not considered in the present work. Also, the reason why $Co_3O_2BO_3$ does not present a similar structural transition remains to be understood.

References

[1] J.P. Attfield, J.F. Clarke, D.A. Perkins, Physica B 180–181 (1992) 581–584.
[2] J.C. Fernandes, R.B. Guimarães, M.A. Continentino, H.A. Borges, A. Sulpice, J-L. Tholence, J.L. Siqueira, L.I. Zawislak, J.B.M. da Cunha, C.A. dos Santos, Phys. Rev. B **58** (1998) 1–6.
[3] R.B. Guimarães, M. Mir, J.C. Fernandes, M.A. Continentino, H.A. Borges, G. Cernicchiaro, M.B. Fontes, D.R.S. Candela, E.M. Baggio-Saitovitch, Phys. Rev. B 60 (1999) 6617–6622.
[4] M. Mir, R.B. Guimarães, J.C. Fernandes, M.A. Continentino, A.C. Dorigueto, Y.P. Mascarenhas, J. Ellena, E.E. Castellano, R.S. Freitasand, L. Ghivelder, Phys. Rev. Lett. 87 (2001) 1–4 (147201).
[5] M. Mir, Jan Janczakb, Y.P. Mascarenhas, J. Appl. Crystallogr. 39 (2006) 42–45.
[6] J.S. Swinnea, Hugo Steinfink, Am. Mineral. 68 (1983) 827–832.
[7] J.C. Fernandes, R.B. Guimarães, M.A. Continentino, L. Ghivelder, R.S. Freitas, Phys. Rev. B 61 (2000) R850–853.
[8] A.P. Douvalis, A. Moukarika, T. Bakas, G. Kallias, V. Papaefthymiou, J. Phys.: Condens. Matter 14 (2002) 3303–3320.
[9] J. Larrea, D.R. Sánchez, F.J. Littest, E.M. Baggio-Saitovitch, J.C Fernandes, R.B Guimarães, M.A. Continentino, Phys. Rev. B 70 (2004) 1–8 (174452).
[10] J.C. Fernandes, R.B. Guimarães, M.A. Continentino, E.C. Ziemath, L. Walmsley, M. Monteverde, M. Nuñez-Regueiro, J.-L. Tholence, J. Dumas, Phys. Rev. B 72 (2005) 1–5 (075133).
[11] P. Bordet, E. Suard, Phys. Rev. B 79 (2009) 1–7 (144408).
[12] Y. Takéuchi, Takéo Watanabe, T. Ito, Acta Crystallogr. 3 (1950) 98–107;
A detailed description of the ludwigite structure could be found in, in: Howard W. Jaffe (Ed.), Crystal Chemistry and Refractivity, Dover, 1996, pp. 256–259.
[13] R. Norrestam, K. Nielsen, I. Sotofte, N. Thorup, Z. Kristallogr. 189 (1989) 33.
[14] D.C. Freitas, M.A. Continentino, R.B. Guimarães, J.C. Fernandes, J. Ellenaand, L Ghivelder, Phys. Rev. B **77** (2008) 1–8 (184422).
[15] N.B. Ivanova, A.D. Vasilév, D.A. Velikanov, N.V Kazak, S.G. Ovchinnikov, G.A. Petrakovskiiand, V.V. Rudenko, Phys. Solid State 49 (2007) 651–653.
[16] J.P. Attfield, A.M.T. Bell, L.M Rodriguez-Martinez, J.M. Greneche, R.J. Cernick, J.F. Clarke, D.A. Perkins, Nature (London) 396 (1998) 655–658 (In this paper there is a clear comparative discussion beween magnetite and Fe warwickite).
[17] E.J. Verwey, P.W. Haayman, Physica VIII (n.9) (1941) 979–987.
[18] J.P. Attfield, A.M.T. Bell, L.M. Rodrigues-Martinez, J.M. Greneche, R. Retoux, M. Leblanc, R.J. Cernik, J.F. Clarke, D.A. Perkins, J. Mater. Chem. 9 (1999) 205–209.
[19] J.P. Wright, J.P. Attfield, J.P. Radaelli, Phys. Rev. Lett. 87 (26) (2001) 1–4 (266401).
[20] J.P. Wright, J.P. Attfield, J.P. Radaelli, Phys. Rev. B 66 (2002) 1–15 (214422).
[21] M. Matos, J. Solid State Chem. 177 (2004) 4605–4615.
[22] M.-H. Whangbo, H.-J. Koo, J. Dumas, M.A. Continentino, Inorg. Chem. 41 (2002) 2193–2201.
[23] A. Latgé, M.A. Continentino, Phys. Rev. B 66 (2002) 1–5 (94113).
[24] E. Vallejo, M Avignon, Phys. Rev. Lett. 97 (2006) 1–4 (217203).
[25] E. Vallejo, J. Magn. Magn. Mater. 321 (2009) 640–643.
[26] D. Hobbs, G. Kresse, J. Hafner, Phys. Rev. B 62 (17) (2000) 11556–11570.
[27] G. Kresse, J. Hafner, Phys. Rev. B 47 (1993) 558;
G. Kresse, J. Hafner, Phys. Rev. Sect. B B49 (1994) 14251;
G. Kresse, J. Furtmüller, Comput. Mater. Sci. 6 (1996) 15;
G. Kresse, J. Furtmüller, Phys. Rev. B 54 (1996) 11169.